Glass transition temperature of Risø B3 radiochromic film dosimeter and its importance on the post-irradiation heating procedure

Skowyra, Magdalena Maria; Ankjærgaard, Christina; Yu, Liyun; Lindvold, Lars René; Skov, Anne Ladegaard; Miller, Arne

Published in:
Radiation Physics and Chemistry

Link to article, DOI:
10.1016/j.radphyschem.2022.109982

Publication date:
2022

Document Version
Publisher's PDF, also known as Version of record

Radiation Physics and Chemistry 194 (2022) 109982

Contents lists available at ScienceDirect

Radiation Physics and Chemistry

journal homepage: www.elsevier.com/locate/radphyschem

Glass transition temperature of Risø B3 radiochromic film dosimeter and its importance on the post-irradiation heating procedure

Magdalena Maria Skowyra [a,*], Christina Ankjærgaard [a], Liyun Yu [b], Lars René Lindvold [a], Anne Ladegaard Skov [b], Arne Miller [a]

[a] Technical University of Denmark, Department of Health Technology, Frederiksborgvej 399, 4000, Roskilde, Denmark
[b] Technical University of Denmark, Department of Chemical and Biochemical Engineering, Søltofts Plads 227, 2800, Kgs. Lyngby, Denmark

ARTICLE INFO

Keywords:
Risø B3 film
Radiochromic
Dosimeter
Glass transition temperature
Post-irradiation

ABSTRACT

Full-color development and stability of measured absorbance of the commercially used Risø B3 radiochromic film dosimeter can be achieved by applying a post-irradiation heat treatment procedure, typically at 60 °C for 10 min. However, the choice of post-irradiation heating duration and temperature has only been based on a trial and error method, and thus, the thermal stability of the material has not been fully studied before. We show that B3 film undergoes a rapid thermal decomposition of the PVB polymer base at 400 °C, with an initiation of the process at 70 °C. It means that higher irradiation temperatures, which can occur e.g. at high-dose electron beam irradiation, may cause polymer degradation. We also show that the post-irradiation heating temperature agrees with the polymer material's glass transition temperature as measured by differential scanning calorimetry (DSC). The post-irradiation heating procedure successfully removes the film's thermal history. This can be seen as an endothermic peak in the first heating cycle, which becomes smaller for higher irradiation doses. Glass transition temperatures of irradiated and post-irradiation heated B3 film are lower than those of the non-irradiated film, and decrease with increasing the dose. That implies a probable chain scission or degradation of the base polymer upon irradiation using high dose rates with no irradiation temperature control.

1. Introduction

Among radiation dosimetry systems commonly used in the radiation processing industry (ICRU Report 80, 2008), radiochromic-dye films constitute an important and broad group of dosimeters, with FWT-60 (Humpherys and Kantz, 1977), Risø B3 (Miller et al., 1988), CTA (ICRU Report 80, 2008; ISO/ASTM 51650-13, 2013) and GafChromic (McLaughlin et al., 1996) as examples of well-established systems. Their principle of operation is based on a direct color formation or darkening of the material upon absorption of ionizing radiation doses, ranging from around 10 Gy to more than 100 kGy. The FWT-60 (Far West Technology Inc., US) and Risø B3 (Tesa AG, Germany) radiochromic films are freestanding polymer foils of thickness of the order of tens of microns. Both are flexible and colorless prior to irradiation and can be prepared as commercially available dosimeters or cut into desired shapes for absorbed-dose mapping. The absorbed dose is determined from the measurement of the absorbance values at specific wavelengths with a spectrophotometer (McLaughlin et al., 2011) or optical scanner (Helt-Hansen and Miller, 2004).

The chemical structure of the polyvinyl butyral (PVB) polymer used in Risø B3 film can be seen in Fig. 1 (a). PVB is doped with a radiation-sensitive triphenylmethane dye, namely pararosaniline cyanide (*4′,4′,4″-triamino-triphenylaceto-nitrile*), presented in Fig. 1 (b). Upon absorption of ionizing radiation energy, the molecule forms a cyanide radical (CN·), which is quickly scavenged as an anion, and a stable triphenyl methane radical, which acts as a stable chromophore (Bernal-Zamorano et al., 2019) with magenta-like color (McLaughlin, 1966). These deeply colored species have a characteristic absorption band whose intensity is measured spectrophotometrically in the visible spectrum (at 554 nm) (Miller et al., 1988; Helt-Hansen and Miller, 2004). The useful dose range is limited to high-dose applications, with doses in the range of 5–100 kGy (Miller and McLaughlin, 1980), used for e.g. sterilization of medical devices and food irradiation. The B3 film is optically transparent, easy to handle, and has good spatial resolution and reproducibility.

However, the radiation-induced response of B3 film is nonlinear and

* Corresponding author.
E-mail address: magsk@dtu.dk (M.M. Skowyra).

https://doi.org/10.1016/j.radphyschem.2022.109982
Received 9 August 2021; Received in revised form 2 November 2021; Accepted 16 January 2022
Available online 23 January 2022

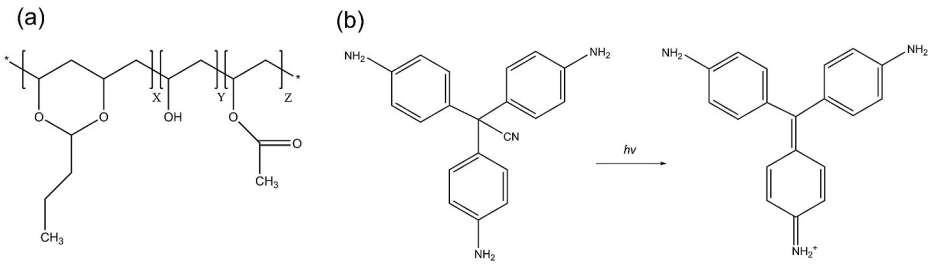

Fig. 1. Chemical structures of: (a) PVB (Carrot et al., 2015), (b) pararosaniline cyanide dye with its radiochromic change induced by ionizing radiation (ICRU Report 80, 2008).

is affected by almost all environmental factors, e.g. temperature during irradiation and handling, relative humidity (water content), UV light (below 375 nm) and time elapsed since manufacture and irradiation (ICRU Report 80, 2008). Due to the combined effects of these and other factors, careful calibration of these systems preferably using in-plant calibration is needed (Miller et al., 1975; McLaughlin, 1989). It has been observed by several authors that the full-color development is not immediate (Miller et al., 1988) and may take up to several hours or even days to reach the correct optical density values (Miller, 1983). Therefore, an additional step needs to be performed after irradiation, namely a post-irradiation heating procedure carried out at 60 °C for 5–10 min (Miller et al., 1988). ASTM Standard Practice for Use of a Radiochromic Dosimetry System (ISO/ASTM 51275-13, 2013) also suggests a heat treatment procedure for faster absorbance stabilization after consulting with a dosimeter manufacturer. The absence of the heating procedure might result in 5–10% lower absorbance levels (Miller et al., 1988) and lead to additional uncertainties. However, once the heat treatment is done, the absorbance varies only ± 2% for up to half a year of storage at room temperature (Miller, 1983). This variance of 2% is included in the uncertainty budget of the dose measurement.

The post-irradiation storage procedures are similar for other radiochromic dosimetry films, with 2 h at 45 °C for GafChromic (Reinstein et al., 1998), 30 min at 80 °C for PVC (Miller and Liqing, 1985), and 5 min at 60 °C for FWT-60 (Abdel-Fattah and Miller, 1996). Thin films are likely to be affected by temperature and humidity because of their large surface-to-volume ratio (Abdel-Fattah and Miller, 1996). Literature shows that the heat treatment of B3 film stabilizes the absorbance readouts (Miller et al., 1975) and decreases the humidity dependence of the dosimeter (Miller, 1983). In our understanding, the heat treatment may also enable a more profound oxygen diffusion in the polymer material (Celina and Quintana, 2018), especially after exposing it to temperatures above its glass transition temperature, T_g. This transition expands the free volume in the polymer (Ravve, 2012) and hence it can contain more diffusing molecules (Swapna et al., 2020). However, no comprehensive thermal analysis of the B3 film dosimeter with a focus on the effectiveness of the post-irradiation heating procedure has been performed so far.

Our study aims to look at the B3 film dosimeter film from a polymer point of view and to study its thermal stability and transitions in order to understand the post-irradiation heating procedure. We present the changes in weight related to temperature changes using thermogravimetric analysis (TGA) for both non-irradiated and irradiated films. The influence of post-irradiation heating on polymer decomposition was also studied. The endo- and exothermic processes and changes in heat capacity were analyzed using differential scanning calorimetry (DSC) with a special focus on changes in glass transition temperatures. Here as well, the measurements of both non-irradiated and irradiated, non-post-irradiation-heated and heated films were compared. We show how the post-irradiation glass transition temperature varies with time and how it is influenced by radiation dose. Lastly, we assess the current post-irradiation procedure based on the obtained results.

Table 1
Specification of the irradiation process parameters.

Nominal irradiation dose (kGy)	Beam current (mA)	D_μ (kGy)	Total uncertainty, $k = 2$, (%)
10	1.55	**10.8**	10.7
30	4.64	**32.2**	10.7
50	7.73	**53.2**	10.7
100	9.28	**112.9**	10.8

2. Materials and methods

2.1. B3 film

The dosimeter used for this study was the Risø B3 radiochromic film. It is a commercially available film made of a terpolymer polyvinyl butyral (PVB) having 11.5–13.5 mol% polyvinyl alcohol content (Butvar® B-76, Solutia Inc (2006), of batch B3-09 1.15.3 (Risø HDRL)), with an average thickness of approximately 17 μm. Before use, pieces of the film were stored under ambient conditions at 22 ± 3 °C and with active protection against UV exposure. Before irradiation, the material was transparent and colorless, and it became magenta-colored upon irradiation, with the intensity of the color dependent on the absorbed dose.

2.2. Irradiation

Irradiations were carried out on a low-energy electron beam accelerator at Risø HDRL (*e-beam*, EBLab-200, COMET AG) using 200 kV, maintaining 15 m/min conveyor speed, 15 mm air gap between dosimeters and electron beam window and at laboratory conditions with an average temperature of 21 °C and a humidity level between 30 and 50%. Calibration is performed at these specific conditions by comparison with alanine film reference dosimeters with traceability to national standards. Four different nominal doses were applied: 10, 30, 50 and 100 kGy of beam currents specified in Table 1. The films were placed on a polystyrene plate, together with three alanine reference dosimeter films and two types of temperature control labels: one sensitive for the range of 37–65 °C (RS PRO Components Ltd.) and the other sensitive from 27.5 °C up to 65 °C (Gex Corporation). For films irradiated with doses of 50 and 100 kGy, an additional temperature control label for the temperature range of 71–110 °C (RS PRO Components Ltd.) was added. The geometry of the irradiation process can be seen in Fig. 2, showing (a) before and (b) after irradiation. Irradiation to 50 and 100 kGy resulted in a significant temperature increase up to 40 °C and 65 °C, respectively, measured using the temperature labels. The temperature increase of PVB material is estimated to be approximately 0.74 °C for every 1 kGy of absorbed dose (Wilski, 1969; Carrot et al., 2015). Measured temperature values were in reasonable agreement with the estimations.

2.3. Alanine-EPR calibration

Since B3 film is used as a routine dosimeter, the response had to be

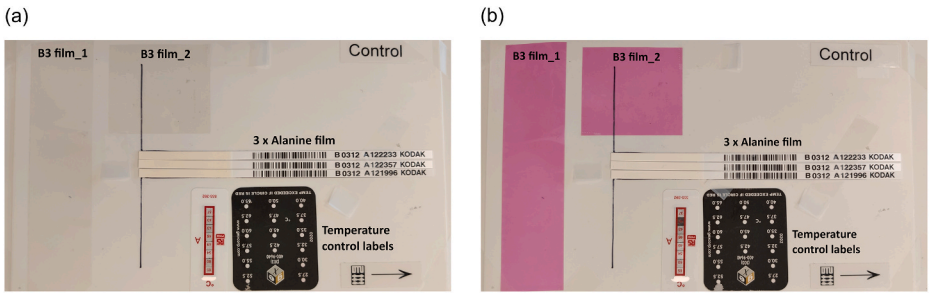

Fig. 2. Irradiation setup: a) before, and b) after irradiation with 50 kGy using a 200 kV e-beam. Dose control was performed using alanine films and temperature labels. The arrow on the plate indicates the direction of movement under the e-beam.

calibrated using a reference dosimetry system. Here, alanine reference dosimeter films (Risø HDRL) with the dose traceable to the national standards at the National Physical Laboratory, UK, were used. Alanine films were chosen as the most appropriate reference dosimeter for low-energy e-beam dose measurements. For each irradiation, three alanine film dosimeters (Kodak, batch B0312), of a thickness of 130 μm, were placed next to each other. The actual dose was estimated in terms of D_μ, the dose in the first micron of the absorbing material, using a procedure reported in the literature (Helt-Hansen et al., 2010). A summary of the irradiation parameters and resulting D_μ doses can be seen in Table 1. From here on in the text, only nominal doses are given.

2.4. Post-irradiation heating procedure

Right after the irradiation, a piece of each of the irradiated B3 film, denoted later in the text as *processed* B3 film, was placed in the oven at a constant temperature of 60 °C for 10 min. The rest of the film, denoted *non-processed* film, was kept in the laboratory conditions up to the measurement time.

2.5. Thermogravimetric analysis (TGA)

The measurements of weight loss versus temperature and thermal stability of the B3 dosimeter film were performed on a Discovery TGA (TA Instruments, US). The TGA data also helped in selecting experimental conditions for differential scanning calorimetry measurements. 5–7 mg of the B3 film was placed in the platinum pan and heated in a nitrogen atmosphere from room temperature to 900 °C, with a heating rate of 10 °C/min. The readout of the sample weight versus temperature was performed every 0.01 s. The analysis was performed on both non-irradiated and irradiated film (non-processed and processed), and the results were analyzed by the TRIOS software (TA Instruments). The accuracy of weight determination was $< \pm 0.1\%$ of a measured value.

2.6. Differential scanning calorimetry (DSC)

Differential scanning calorimetry (DSC) was conducted to measure the heat flow produced in the sample when it was heated, cooled or held at a constant temperature. Consequently, the phase transitions as a function of temperature were determined. Approximately 2–5 mg of B3 film was accurately weighed, cut into small pieces using a scalpel and placed in the T_{zero} aluminum hermetic pan. The weight of the samples was determined with the accuracy of ± 0.01 mg. Both non-irradiated and irradiated (non-processed and processed) material was tested. DSC measurements were performed in a nitrogen atmosphere on a Discovery TGA (TA Instruments, US) with a heating and cooling rate of 10 °C/min. Each measurement consisted of a first heating step from −90 °C to 200 °C (isothermal at −90 °C for 5 min), a cooling step from 200 °C to −90 °C (isothermal at −90 °C for 5 min), and a second heating step from −90 °C to 300 °C. The validation enthalpy difference was $< \pm$ 0.1%.

Table 2
Glass transition temperature measurement: sources of error and estimated reproducibility.

Source	Reproducibility of measurement	Comments
Mass of the specimen	0.02%	Reproducibility of the balance
Putting the sample into the crucible	negligible	The static charge on the surface was removed with an anti-static gun (Zerostat3)
Thermal contact with the crucible	0.5%	Estimated (Fedelich et al., 2016)
Heating rate	negligible	Did not change between measurements
Gas and gas flow	negligible	Adjusted under the same conditions
Adjustment	0.1 %	Uncertainty of the calibration material
Baseline definition	3%	Choice of a correct range of temperatures (Fedelich et al., 2016)
T_g determination	1%	Temperature reproducibility of the equipment

The glass transition temperature (T_g) of B3 film was determined from DSC curves as an endothermic transition from the amorphous glassy state into the viscous rubbery state (Ravve, 2012) by means of a second heating scan. T_g was determined using the TRIOS software (TA Instruments) as a midpoint (halfway point) temperature of the jump in heat capacity in the chosen temperature range (ASTM E1356-08, 2008). The temperature accuracy of the equipment was ± 0.1 °C and the temperature precision ± 0.05 °C.

Estimation of the reproducibility of the glass transition temperature measurement was made based on four main influence factors: sample preparation, method development, measurement (instrument), and evaluation (baseline type and temperature limits) (Mettler Toledo, n.d.). The individual uncertainty components at $k = 1$ are given in Table 2.

The combined uncertainty for the T_g was thus:

$$\sqrt{(0.02\%)^2 + (0.5\%)^2 + (0.1\%)^2 + (3\%)^2 + (1\%)^2} = 3.20\%$$

3. Results and discussion

3.1. Thermogravimetric analysis

Before beginning the DSC tests, a TGA measurement of a non-irradiated sample was run to determine the decomposition temperature of the polymer. The weight loss of non-irradiated B3 film versus temperature can be seen in Fig. 3 (a). The thermal treatment causes the mass of PVB to change continuously, with the first 1.25% mass loss at 70 °C, followed by another 1.46% weight loss at 250 °C, as presented in Fig. 3 (b) and in Table 3. Those two weight changes might be due to volatile loss or plasticizer evaporation. A rapid weight loss of the material starts to occur at around 380 °C, followed by a complete decomposition at 400 °C, where the decomposition of the butyral ring occurs,

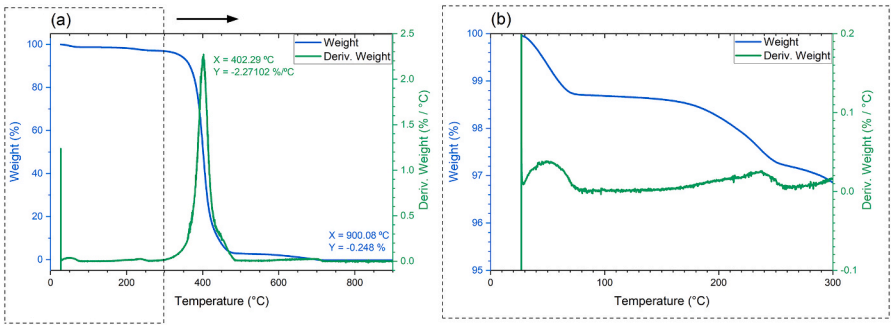

Fig. 3. (a) Non-irradiated B3 film: TGA curve: blue-weight (%) vs temperature (°C); green – the derivative of weight with respect to temperature (%/°C). Curves X (temperature) and Y (weight/deriv. weight) coordinates are also depicted. (b) The zoom-in of Fig. 3 (a) for temperatures below 300 °C.

Table 3
Absolute (mg) and relative (%) weight loss vs temperature for: non-irradiated film, irradiated (200 keV, 30 kGy) non-processed film and irradiated (200 keV, 30 kGy) processed film. T_0 is the temperature at the beginning of each experiment.

	Irradiated: non-processed		Irradiated: non-processed film		Irradiated: processed film	
	Weight (mg)	Weight (%)	Weight (mg)	Weight (%)	Weight (mg)	Weight (%)
T_0	4.782	100	5.99	100	6.98	100
70 °C	4.723	98.755	5.929	98.978	6.954	99.614
250 °C	4.653	97.288	5.826	97.266	6.842	98.017
400 °C	2.53	52.897	3.249	54.242	3.823	54.767

leading to the formation of products, such as butyraldehyde, and butenal and acetic acid from the acetate groups (Carrot et al., 2015). Also, benzene and toluene are produced due to the decomposition of polyene products (Dhaliwal and Hay, 2002; Zanjanijam et al., 2018; Liau et al., 1996). In the end, after heating to 900 °C, there are no residues left in the crucible, leaving the material fully degraded.

A similar analysis was conducted for irradiated B3 film (30 kGy), both for non-processed and processed film, which can be seen in Fig. 4 (a) and Table 3. The weight loss for temperatures below 300 °C is also presented in Fig. 4 (b), where the mass loss is slightly smaller for the processed film. However, the thermal degradation of irradiated polymer film does not strongly differ from the non-irradiated one, which indicates no significant material changes during the irradiation process. Based on these results, the upper limit for DSC measurement was chosen to be 200 °C in the 1st cycle and 300 °C in the 2nd. PVB film should not be exposed to temperatures higher than 380 °C and ideally not higher than 70 °C in order to prevent its decomposition. That being said, irradiations with very high doses, where no temperature control is introduced, can sometimes lead to a significant temperature increase that might cause a partial degradation of the PVB film. We observed that films irradiated to 100 kGy using e-beam became wrinkled and creased, as illustrated in Fig. 5 (a). However, the effect was not as intense once the films were

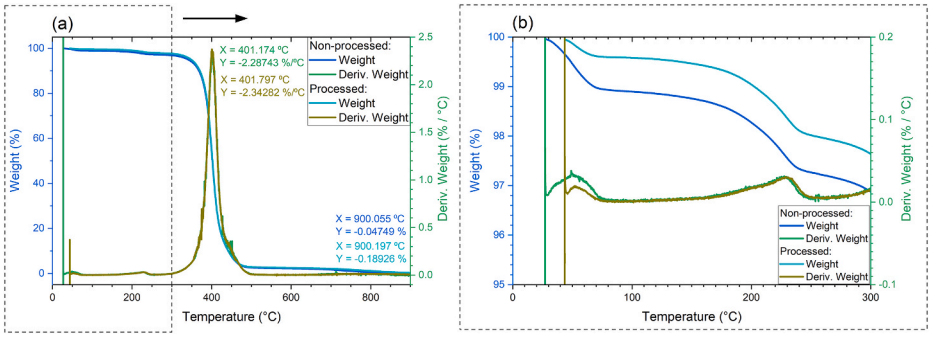

Fig. 4. (a) TGA curves of irradiated B3 film (200 kV, 30 kGy) of non-processed and processed film. Blue curves: weight (%) vs temperature (°C); green: the derivative of weight with respect to temperature (%/°C). Curves X (temperature) and Y (weight/deriv. weight) coordinates are also depicted. (b) The zoom-in of Fig. 4 (a) for temperatures below 300 °C.

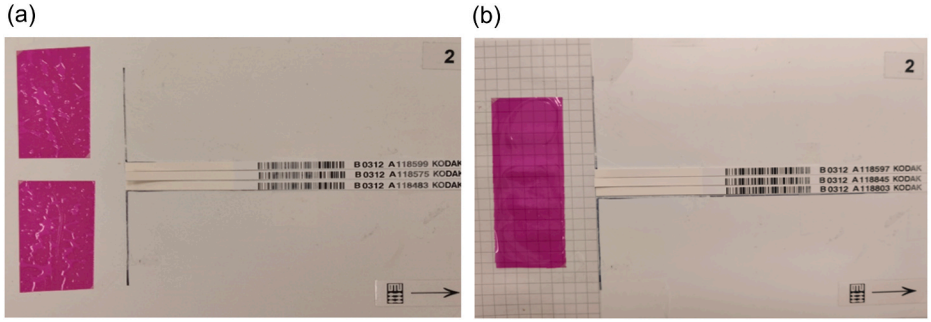

Fig. 5. The irradiation setup of B3 film irradiated with 100 kGy using a 200 kV e-beam. B3 film was placed: (a) on a polystyrene back plate, (b) on a paper substrate.

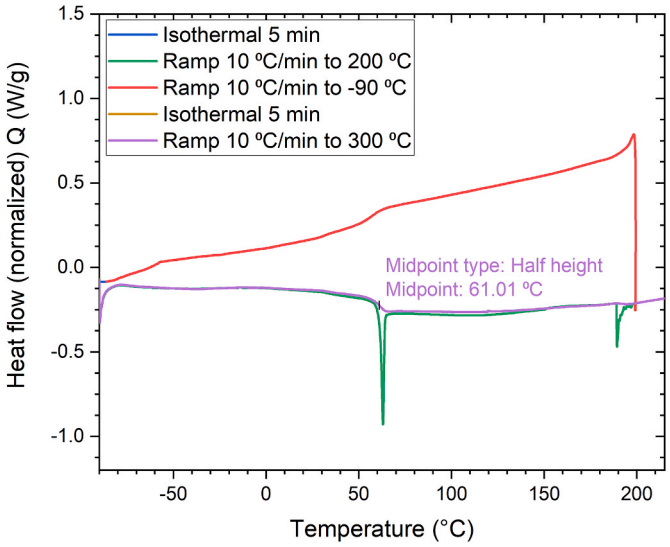

Fig. 6. Non-irradiated B3 film: DSC curves: green- 1st heating cycle, red – cooling step, violet – 2nd heating cycle. T_g value (midpoint) is presented on the graph.

initially placed on a different substrate, e.g. paper, as can be observed in Fig. 5 (b). The reason for the effect is likely to be volatiles not able to dissipate through the polystyrene back plate, while they dissipate easily through the paper. TGA was also performed for those films irradiated with 100 kGy (200 keV e-beam), both non-processed and processed, as can be seen in Fig. S1 in ESI. No significant differences in the initial decomposition were observed as compared with Fig. 4.

3.2. Differential scanning calorimetry

The measurement of the heat flow versus temperature of the non-irradiated B3 film can be seen in Fig. 6. A clear endothermic peak, with its minimum around 60 °C, is visible during 1st heating cycle. It indicates an unknown thermal history of the film, which is erased with the first heating step and leaves the readout of the glass transition temperature in the second heating cycle much more distinct. The calculated T_g of non-irradiated B3 film was 61.01 °C, which is in close agreement with the literature value of 59 °C for pure PVB polymer (Nielsen, 1993). However, theoretical T_g values of PVB can vary significantly, depending on the amount of plasticizers used (Dhaliwal and Hay, 2002) and the content of vinyl alcohol in the polymer chain (Carrot et al., 2015; Zhou et al., 1997).

The analysis was also conducted for the irradiated film, both non-processed and processed, and DSC curves can be seen in Fig. 7 (a) and (b). The endothermic peak, even though a bit weaker than the one of non-irradiated film, is still present in the irradiated, non-processed film (Fig. 7 a), whereas after the post-irradiation procedure it completely disappears (Fig. 7 b). This observation may be explained as the thermal treatment after irradiation (10 min at 60 °C) causes the kinetic energy of the molecules to increase, leading to increased long-range molecular motions, thereby bringing greater rotational freedom and an increase in the free volume (Stevens, 1999). When the polymer film is kept at this temperature, it loses its glasslike properties and can be identified as a rubber. Hence, it has enough time to reach thermal equilibrium and erase the initial thermal history, seen as an endothermic peak. This finding indicates that the post-irradiation treatment temperature of films (60 °C) used for many years is approximately equal to the T_g of the PVB polymer film.

Additionally, the glass transition temperature slightly decreases after irradiation - to around 55 °C – and recovers to the value of the non-irradiated film for processed samples of 59 °C. This phenomenon is possibly correlated with the weaker color formation, and consequently initial lower optical density values for non-processed films, which ultimately approach higher values. The differences in color formation for films irradiated with different doses can be seen in Fig. 8 and their quantitative values in Table 4. The color difference is presented as a percentage change between non-processed and processed film, measured using the RisøScan software (Helt-Hansen and Miller, 2004). The post-irradiation heat treatment develops the color to a level that is 5–15% higher than what is reached by normal storage in laboratory conditions (Miller et al., 1988), and stays stable within the measurement uncertainties for more than 20 months after heating (Miller and Helt-Hansen, 2010). The slow development of the color is more pronounced at low irradiation temperature and low relative humidity during irradiation (Abdel-Fattah and Miller, 1996). The color formation seems to also be affected by the amount of oxygen present during the irradiation process: irradiation of B3 dosimeter film in vacuum results in no initial color formation up to the exposure to air, after which the reaction happens in a matter of seconds.

3.3. 1st heating cycle of non-processed and processed B3 films

DSC analysis was performed for film irradiated with different high doses, both non-processed (a) and processed (b), and their 1st heating cycles are compared in Fig. 9. For the non-processed film, Fig. 9 (a), there is a clear tendency of the endothermic peak to decrease and shift its minimum to lower temperatures with an increase of dose. Ultimately, it fully disappears for the highest dose of 100 kGy. This behavior shows that the films irradiated with different doses also possess different thermal histories, which are due to the increase of the temperature during the irradiation process for higher doses using e-beam. Molecular relaxations cause the release of any internal stresses as well (TA

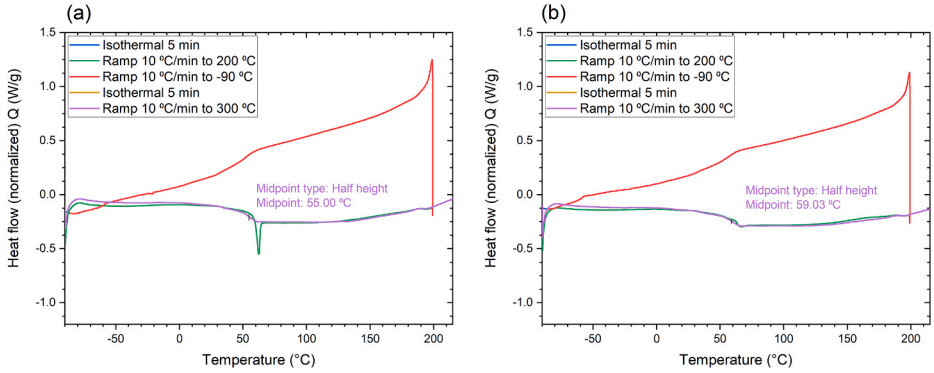

Fig. 7. Irradiated B3 film (30 kGy) - DSC curves of: (a) non-processed, and (b) processed film. Green- 1st heating cycle, red – cooling step, violet – 2nd heating cycle. T_g values (midpoints) are determined and presented on the graphs.

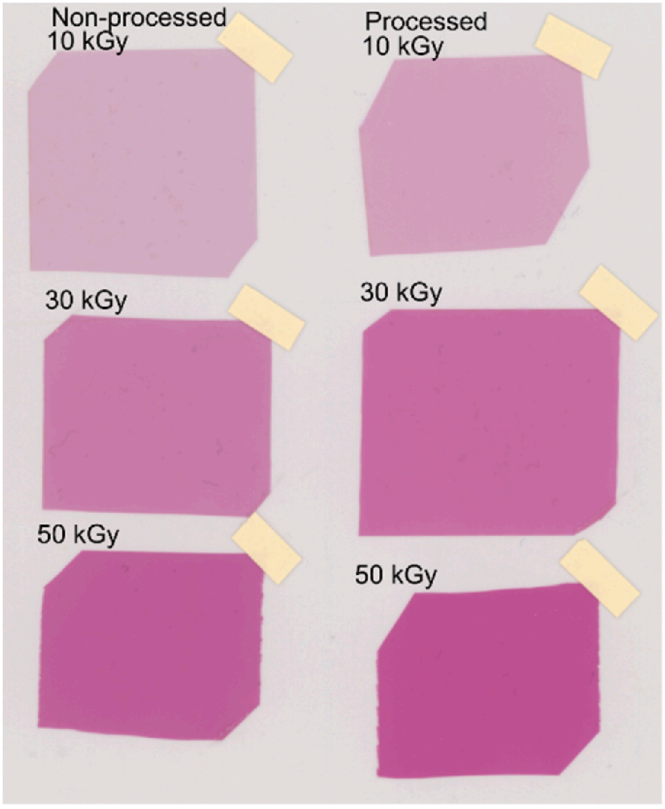

Fig. 8. Post-irradiation heat treatment procedure's influence on the color formation of irradiated B3 film. Left: non-processed film, right – processed film (60 °C, 10 min). Scan from the RisøScan software.

Table 4
Post-irradiation heat treatment procedure's influence on the color formation of irradiated B3 film. The response was measured as a gray value (1–255) using the RisøScan software.

Nominal dose (kGy)	Non-processed film (AU)	Processed film (AU)	Percentage change (%)
10	83.9 ± 1.1	96.4 ± 1.2	14.90 ± 2.08
30	133.6 ± 1.0	148.8 ± 1.0	11.38 ± 1.12
50	162.4 ± 1.2	172.5 ± 1.0	6.22 ± 1.00

Intruments, n.d.). Compared with the processed film, Fig. 9 (b), there are no endothermic peaks visible for any of the irradiated films, which indicates complete removal of the thermal history of the material by applying the post-irradiation procedure. Stresses built into the material as a result of post-irradiation processing, handling or thermal history are released when the material is heated through its glass transition (TA Intruments, n.d.). The differences in heat flow values may be due to the different masses of measured samples, since very small amounts (2–5 mg) of highly electrostatic B3 film were difficult to weigh and place in the aluminum pan, or due to the asymmetry between the power of the reference heater and the sample heater.

3.4. Post-irradiation glass transition temperature variations

We also studied the dose-dependency on the glass transition temperature of processed B3 film, which can be seen in Fig. 10. All irradiated films are characterized by a lower glass transition temperature than that of non-irradiated material, the latter indicated by the dashed line in the figure. The reason for that could be some chain scission and degradation of the polymer matrix, which lower the molecular weight and favor molecular mobility, consequently causing a decrease of the transition temperatures (Ferry et al., 2020). Furthermore, the higher the dose, the lower the glass transition temperature of the tested material. The trend takes the form of a linear curve. This observation might be valid for users performing irradiations using electron beams, where very high dose rates are applied and the temperature is usually not controlled during the process. It would be of interest for the dosimetry community

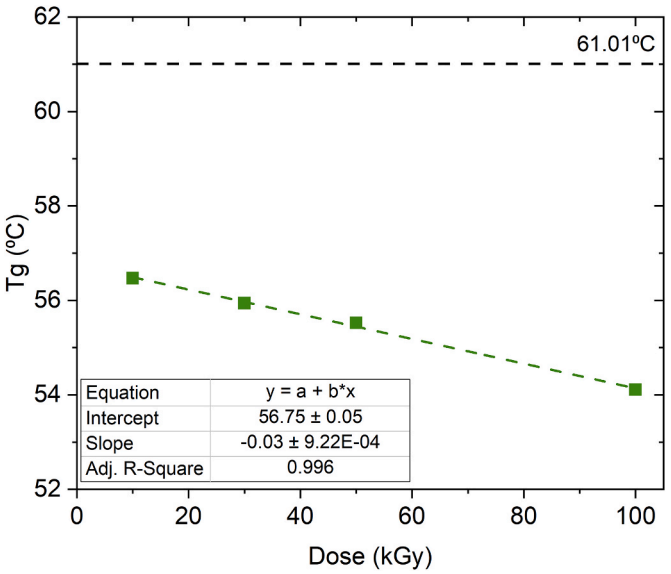

Fig. 10. T_g of processed B3 film irradiated with different doses. The black dashed line presents the T_g of a non-irradiated film. The data points were fitted with a linear function, of parameters presented in the Table.

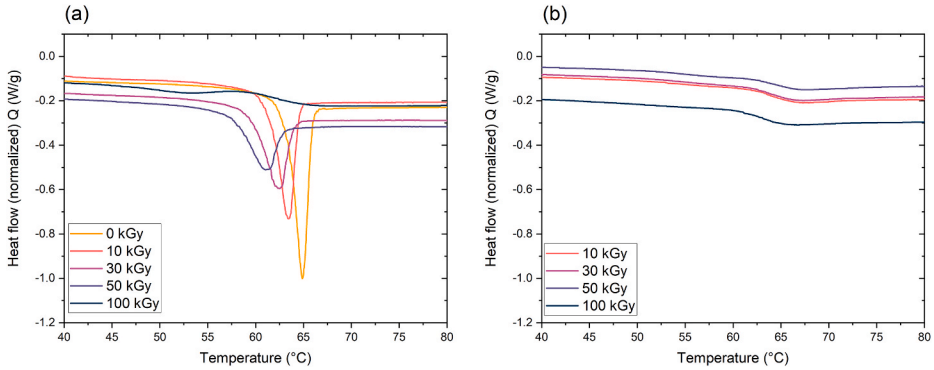

Fig. 9. DSC of B3 film - 1st heating cycles of: (a) non-processed film - endothermic peak dependency on the irradiation dose, (b) processed film - endothermic peak not present. Nominal doses are presented.

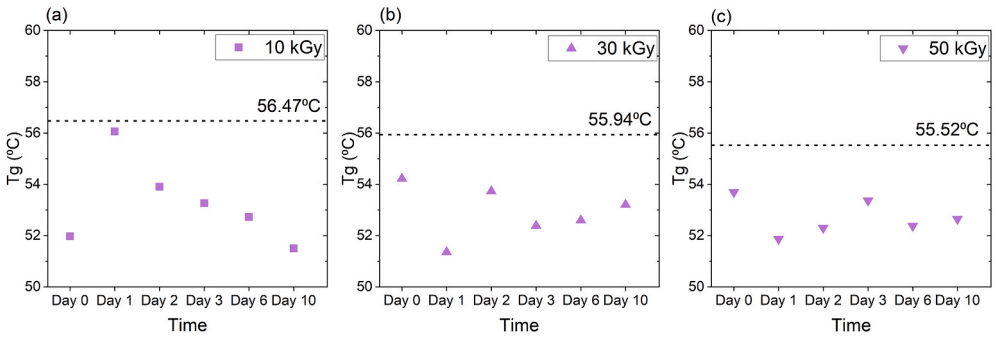

Fig. 11. Post-irradiation glass transition temperature variations of non-processed B3 films irradiated with: (a) 10 kGy, (b) 30 kGy, (c) 50 kGy. The dashed lines present the values of processed films irradiated with the same doses respectively.

to study this property of the B3 films but using gamma irradiation at a constant temperature, thereby avoiding the temperature effects.

One of the hypotheses was also to test the glass transition temperature changes with time, during the first few days after irradiation, to monitor if the values will approach the initial T_g of non-processed, non-irradiated film. Glass transition temperatures of the irradiated, non-processed film was measured for a few days after irradiation and the results are presented in Fig. 11 for (a) 10, (b) 30, and (c) 50 kGy. It was expected that the T_g would ultimately shift to the value of corresponding processed films (dashed lines). However, no clear tendency was observed, but all the irradiated, non-processed films had lower T_g than their processed equivalents. The average T_g of non-processed films presented in Fig. 11 was calculated to be 52.95 °C, with reproducibility of ± 2.20 °C (at $k = 2$), and the average T_g of processed films was 55.98 °C, with reproducibility of ± 0.78 °C (at $k = 2$). The estimated combined uncertainty (as described in 2.6.) was of the order of calculated reproducibility, with ± 1.69 °C and ± 1.79 °C for non-processed and processed film, respectively. This demonstrates that, within the standard deviation of $k = 2$, the T_g of non-processed films was only slightly lower than T_g of processed films.

It should be also noted that, generally, the glass transition temperature of polymers is rather diffuse and extends over a range of temperatures, whose magnitude depends on the polydispersity of the polymer and is defined by several conditions (Ebewele, 2000). Hence, the results presented in this paper will be only valid for the specific conditions chosen during DSC measurements, which were kept constant during the experiments, like e.g. type of reference pan, ramp rate, purge gas, and may greatly vary for different heating or cooling rates, analysis methods, baseline definitions or measurement techniques.

3.5. Assessment of post-irradiation procedure

The post-irradiation procedure of B3 dosimeter film used empirically for several years seem to be a successful approach to stabilize the optical density measurement of the B3 dosimeter film. Both the temperature and time of the heat treatment were chosen based on a trial and error method but here we demonstrate that the choice was not accidental – it matches the glass transition temperature of the PVB polymer film. For the B3 dosimeter film this means that while being at room temperature (intended work environment), molecular chains of amorphous polymer are frozen in place and atoms undergo only low-amplitude vibrational motion about these positions. As the temperature is increased, the amplitude of these vibrations becomes greater, reducing the effectiveness of the secondary intermolecular bonding forces, and enhancing the cooperative nature of the vibrations between neighboring atoms. At the glass transition temperature, chain segments acquire sufficient energy to overcome intermolecular restraints and undergo rotational and translational motion, substantially expanding the free volume (Ebewele, 2000; Ravve, 2012). This facilitates the flow of oxygen or residual alcohol molecules present in the system (Lee, 1980; Cohen and Turnbull, 1959), causing the stabilizing effect, and allowing the color-formation reaction to be completed faster. The time duration of the heating procedure remains to be optimized, but it is assumed that thin-film dosimeters change temperature quickly after exposure to a heat source and 10 min time is likely to be sufficient (Abdel-Fattah and Miller, 1996).

4. Conclusions

The thermal analysis of B3 radiochromic dosimetry films revealed that the PVB polymer base material starts undergoing partial decomposition at 70 °C, following by 200 °C, and a complete weight loss at 400 °C, both for non-irradiated and irradiated films. The measured glass transition temperature of non-irradiated B3 film was comparable to the literature value of the polymer matrix (PVB) and was approximately 61 °C. The non-processed films characterize the presence of an endothermic peak in the 1st heating cycle, which decreased with dose (and temperature) and completely disappear for material processed at 60 °C for 10 min. This observation confirms the effectiveness of the post-irradiation heating procedure, which eliminates the thermal history of the dosimeter film. The glass transition temperature of the irradiated, non-processed film was lower than the one measured for processed film, with no clear tendency of change with time. Moreover, the measurements of T_g for processed film irradiated with different doses showed that the higher the dose the lower the T_g, with the irradiated material always having values lower than the non-irradiated film. It is concluded that the current post-irradiation heating procedure is an excellent way of stabilizing the color formation of the B3 dosimeter film. It might be of interest to investigate the thermal properties of other dosimeter films, such as FWT-50, CTA or GafChromic, that also show a time-dependent response.

Credit authorship contribution statement

Magdalena Maria Skowyra: Conceptualization, Formal Analysis, Investigation, Visualization, Writing - Original Draft, Christina Ankjærgaard: Investigation, Supervision, Liyun Yu: Methodology, Validation, Investigation, Lars René Lindvold: Conceptualization, Project Administration, Supervision, Anne Ladegaard Skov: Conceptualization, Supervision, Arne Miller: Conceptualization, Supervision.

Declaration of competing interest

The authors declare that they have no known competing financial interests or personal relationships that could have appeared to influence the work reported in this paper.

Acknowledgments

DTU Chemical Engineering for permission to use their TGA and DSC equipment. Engineer M. Bailey for help with alanine dosimetry

measurements and calibration.

Appendix A. Supplementary data

Supplementary data to this article can be found online at https://doi.org/10.1016/j.radphyschem.2022.109982.

References

Abdel-Fattah, A.A., Miller, A., 1996. Temperature, humidity and time. Combined effects on radiochromic film dosimeters. Radiat. Phys. Chem. 47 (4), 611–621. https://doi.org/10.1016/0969-806X(95)00037-X.

ASTM E1356-08, 2008. Standard Test Method for Assignment of the Glass Transition Temperatures by Differential Scanning Calorimetry. ASTM International. https://doi.org/10.1520/E1356-08.

Bernal-Zamorano, M.R., Sanders, N.H., Lindvold, L., Andersen, C.E., 2019. Radiochromic and radiofluorogenic solid state polymer dosimeter; a third signal: electron Paramagnetic Resonance (EPR). Radiat. Phys. Chem. 161, 72–76. https://doi.org/10.1016/j.radphyschem.2019.04.008.

Carrot, C., Bendaoud, A., Pillon, C., 2015. Polyvinyl Butyral. In *Handbook Of Thermoplastics*. https://doi.org/10.1201/b19190-4.

Celina, M.C., Quintana, A., 2018. Oxygen diffusivity and permeation through polymers at elevated temperature. Polymer 150, 326–342. https://doi.org/10.1016/j.polymer.2018.06.047.

Cohen, M.H., Turnbull, D., 1959. Molecular transport in liquids and glasses. J. Chem. Phys. 31 (5), 1164–1169. https://doi.org/10.1063/1.1730566.

Dhaliwal, A.K., Hay, J.N., 2002. The characterization of polyvinyl butyral by thermal analysis. Thermochim. Acta 391, 245–255. https://doi.org/10.1016/S0040-6031(02)00187-9.

Ebewele, R.O., 2000. Chapter 4: thermal transitions in polymers. In: Polymer Science and Technology. CRC Press, Boca Raton. https://www.taylorfrancis.com/chapters/mono/10.1201/9781420057805-7/thermal-transitions-polymers-robert-ebewele?context=ubx&refId=cb281b7d-806b-44d3-bb0b-7e572cc58e1e.

Fedelich, N., Hammer, A., Hempel, E., Jing, N., Riesen, R., Schawe, J., Wrana, C., 2016. Thermal analysis in Practice - tips and hints. Mettler Toledo 2, 1–48. Retrieved August 1, 2021, from. https://www.mse.ucr.edu/sites/g/files/rcwecm1241/files/2019-02/Mettler Toledo Tips and Hints.pdf.

Ferry, M., Roma, G., Cochin, F., Esnouf, S., Dauvois, V., Nizeyimana, F., et al., 2020. Polymers in the Nuclear Power Industry. Comprehensive Nuclear Materials, second ed., vol. 3, pp. 545–580. https://doi.org/10.1016/B978-0-12-803581-8.11616-9

Helt-Hansen, J., Miller, A., 2004. RisøScan-a new dosimetry software. Radiat. Phys. Chem. 71, 359–362. https://doi.org/10.1016/j.radphyschem.2004.03.033.

Helt-Hansen, J., Miller, A., Sharpe, P., Laurell, B., Weiss, D., Pageau, G., 2010. Dμ-A new concept in industrial low-energy electron dosimetry. Radiat. Phys. Chem. 79, 66–74. https://doi.org/10.1016/j.radphyschem.2009.09.002.

Humpherys, K.C., Kantz, A.D., 1977. Radiochromic: a radiation monitoring system. Radiat. Phys. Chem. 9, 737–747. https://doi.org/10.1016/0146-5724(77)90186-8.

ICRU Report 80, 2008. Journal of the ICRU, vol. 8. https://doi.org/10.1093/jicru/ndn031.

TA Intruments. (n.d.). Interpreting Unexpected Events and Transitions in DSC Results. Retrieved August 1, 2021, from http://www.tainstruments.com/pdf/literature/TA039.pdf.

ISO/ASTM 51275-13, 2013. Standard Practice for Use of a Radiochromic Film Dosimetry System. https://doi.org/10.1520/ISOASTM51275-13.

ISO/ASTM 51650-13, 2013. Standard Practice for Use of a Polymethylmethacrylate Dosimetry System. https://doi.org/10.1520/ISOASTM51650-13.

Lee, W.M., 1980. Selection of barrier materials from molecular structure. Polym. Eng. Sci. 20 (1), 65–69. https://doi.org/10.1002/pen.760200111.

Liau, L.C.K., Yang, T.C.K., Viswanath, D.S., 1996. Mechanism of degradation of poly (vinyl butyral) using thermogravimetry/fourier transform infrared spectrometry. Polym. Eng. Sci. 36 (21), 2589–2600. https://doi.org/10.1002/pen.10659.

McLaughlin, W.L., 1966. Microscopic visualization of dose distributions. Int. J. Appl. Radiat. Isot. 17 (2), 85–96. https://doi.org/10.1016/0020-708X(66)90053-6.

McLaughlin, W.L., 1989. Reference dosimetry and measurement quality assurance. Appl. Radiat. Isot. 40 (10–12), 945–951. https://doi.org/10.1016/0883-2889(89)90021-X.

McLaughlin, W.L., Puhl, J.M., Al-Sheikhly, M., Christou, C.A., Miller, A., Kovacs, A., Wojnarovits, L., Lewis, D.F., 1996. Novel radiochromic films for clinical dosimetry. Radiat. Protect. Dosim. 66 (1–4), 263–268. https://doi.org/10.1093/oxfordjournals.rpd.a031731.

McLaughlin, W.L., Miller, A., Kovács, A., Mehta, K.K., 2011. Dosimetry methods. In: Handbook of Nuclear Chemistry, pp. 2287–2318. https://doi.org/10.1007/978-1-4419-0720-2_49.

Mettler Toledo. (n.d). Thermal Analysis UserCom 30. Retrieved August 1, 2021, from https://www.mt.com/dk/da/home/library/usercoms/lab-analytical-instruments/thermal-analysis-usercom-30.html.

Miller, A., 1983. Dosimetry for Electron Beam Applications. Risø National Laboratory. No.2401. 4000 Roskilde, DK. https://orbit.dtu.dk/en/publications/c9f2fb19-411a-432c-af99-39395719415f.

Miller, A., Helt-Hansen, J., 2010. Technical Note E1: Stability of Response of GEX DoseStix Dosimeters Heated after Irradiation at Different Temperatures and Different Times. Retrieved from. https://www.healthtech.dtu.dk/english/services-and-products/hdrl/technical-notes.

Miller, A., Liqing, X., 1985. Properties of Commercial PVC Films with Respect to Electron Dosimetry. Risø National Laboratory. No.2508. 4000 Roskilde, DK.

Miller, A., McLaughlin, W.L., 1980. On a Radiochromic Dye Dosemeter, No.2254. Risø National Laboratory, pp. 1–34, 4000 Roskilde, DK. https://orbit.dtu.dk/en/publications/on-a-radiochromic-dye-dosemeter.

Miller, A., Bjergbakke, E., McLaughlin, W.L., 1975. Some limitations in the use of plastic and dyed plastic dosimeters. Int. J. Appl. Radiat. Isot. 26 (10), 611–620. https://doi.org/10.1016/0020-708X(75)90079-4.

Miller, A., Batsberg, W., Karman, W., 1988. A new radiochromic thin-film dosimetry system. Radiat. Phys. Chem. 31 (4–6), 491–496. https://doi.org/10.1016/1359-0197(88)90216-0.

Nielsen, L.E., 1993. Mechanical Properties of Polymers and Composites, vol. 2. https://doi.org/10.1201/b16929.

Ravve, A., 2012. Principles of Polymer Chemistry, third ed. https://doi.org/10.1007/978-1-4614-2212-9

Reinstein, L.E., Gluckman, G.R., Meek, A.G., 1998. A rapid colour stabilization technique for radiochromic film dosimetry. Phys. Med. Biol. 43, 2703–2708. https://doi.org/10.1088/0031-9155/43/10/001.

Solutia Inc, 2006. Butvar: Polyvinyl Butyral Resin. Properties and Uses. Pub. No. 2008084E, 1–28. Retrieved from. http://www.butvar.com.

Stevens, M.P., 1999. Polymer Chemistry: an Introduction, third ed. Oxford University Press, New York.

Swapna, V.P., Abhisha, V.S., Stephen, R., 2020. Polymer/polyhedral oligomeric silsesquioxane nanocomposite membranes for pervaporation. In: Polymer Nanocomposite Membranes for Pervaporation. https://doi.org/10.1016/b978-0-12-816785-4.00009-4.

Wilski, V.H., 1969. Die spezifische Wärme des Polyvinylbutyrals. Angew. Makromol. Chem. 6, 101–108. https://doi.org/10.1002/apmc.1969.050060109.

Zanjanijam, A.R., Hakim, S., Azizi, H., 2018. Rheological, mechanical and thermal properties of the PA/PVB blends and their nanocomposites: structure-property relationships. Polym. Test. 66, 48–63. https://doi.org/10.1016/j.polymertesting.2018.01.006.

Zhou, Z.M., David, D.J., Macknight, W.J., Karasz, F.E., 1997. Synthesis characterization and miscibility of polyvinyl butyrals of varying vinyl alcohol contents. Turk. J. Chem. 21, 229–238. Retrieved August 1, 2021, from. https://journals.tubitak.gov.tr/chem/issues/kim-97-21-4/kim-21-4-1-97081.pdf.